SPATIAL CORRELATION ESTIMATES BASED ON SATELLITE OBSERVATIONS CORRECTED WITH THE PRIOR KNOWLEDGE ON SENSOR DEVICES' TECHNICAL CHARACTERISTICS

G. Arbia, G. Lafratta

1. INTRODUCTION

It is common in many empirical studies to estimate ground characteristics on the basis of satellite images. For instance, in agricultural analysis inventories are often made on the basis of remotely sensed data sometimes corrected with ground surveys (Campbell, 1996). Spatial variability and spatial dependency of data are also often estimated through satellite images. To restrict again to agricultural examples, spatial variability is employed to estimate standard errors of inventory estimates and spatial correlations are used to identify the distance above which dependency is negligible to assist the choice in locating of a systematic grid of samples for ground surveys (Arbia, 1993; Arbia and Lafratta, 1997, 2002).

However, both first and second-order estimates are undermined by the fact that our inference is based on satellite data that are only an approximation of the ground truth, due to the presence of a series of disturbing factors like (e.g.) light scattering, presence of obstacles like clouds, and instrument precision limitations. In particular, we can identify two sources of errors (Haining and Arbia, 1993; Arbia *et al.*, 1998, 1999) namely *location errors* due to the uncertainty we have on the position of a pixel with respect to the corresponding ground truth, and the classical *measurement errors* (or attribute errors) due to device's limitations and other disturbing factors. It is important to remark that in many empirical cases the user can quantify the limits of the instruments in use and therefore can depict a series of worst-case scenarios. Neglecting this information in developing any estimation procedure would then be extremely unwise and doomed to produce unreliable estimates.

In this paper we introduce a procedure to correct the spatial correlation estimates with the prior knowledge on the satellite sensor's technical characteristics. We show that in this way we can derive more reliable estimates. The paper is organized as follows. In Section 2 we introduce a model for the error corruption

---

The authors wish to acknowledge the partial financial contribution of 40% COFIN 2000 by MIUR.

process, that enables us to take into account both location and attribute errors, and we use it to derive the satellite-based spatial correlation as a function of the "true" spatial correlation on the ground. Such a relationship is thus inverted to derive a better approximation of the "ground-truth" pattern of dependence as a function of the satellite-based spatial correlation and of the sensor's (user-specified) technical characteristics. In Section 3 we show the effects of these corrections by referring to a series of illustrative examples based on theoretical isotropic negative exponential correlograms. Furthermore, in Section 4 we assess the efficiency of the proposed correction procedure by simulating a SAR lattice process. Section 5 is devoted to some comments and to concluding remarks.

2. CORRECTION OF SPATIAL CORRELATION ESTIMATES INTRODUCING THE KNOWLEDGE ON SENSOR'S CHARACTERISTICS

Let us define an N_X by N_Y lattice as:

$P = \{1,\ldots,N_X\}\times\{1,\ldots,N_Y\}$.

In this way, every cell in the lattice will be treated as an ordered pair (i, j) for some $i \in \{1,\ldots,N_X\}$ and $j \in \{1,\ldots,N_Y\}$. Let $S_{i,j}$ be the random process on P generating the "ground truth" data and let $Z_{i,j}$ be the process which stochastically generates the corresponding remotely sensed maps. In addition, let us interpret $S_{i,j}$ as a noiseless version of the observed $Z_{i,j}$ by assuming that the satellite observation corrupts the true scene through location and attribute errors as follows: (i) measurement failures due to clouds, obstacles and device's imperfections can be modelled as realizations of an additive white noise spatial process $\varepsilon_{i,j}$ on P; (ii) the satellite can also dislocate S by erroneously assigning to pixel (i, j) a weighted average of observations related to the neighboring pixels $(i + x_t, j + y_t)$, with integers $x_t, y_t \in \mathbb{Z}$, $t = 1,\ldots,T$, so that the error corruption process is modeled applying the following linear transformation:

$$Z_{i,j} = \phi_0 + \phi_1 (S_{i+x_1,j+y_1} \quad \cdots \quad S_{i+x_T,j+y_T})\,\boldsymbol{\theta} + \varepsilon_{i,j} \tag{1}$$

where $\boldsymbol{\theta} \in \mathbb{R}^T$ is a dislocation parameter satisfying

$$\sum_{t=1}^{T} \theta_t = 1 \tag{2}$$

and the pair (i, j) belongs to a set $P' \subset P$, depending on vectors $\mathbf{x}' = (x_1 \quad \cdots \quad x_T)$ and $\mathbf{y}' = (y_1 \quad \cdots \quad y_T)$, whose elements are exactly those coordinates in P for which we have enough data to model $Z_{i,j}$. More thoroughly, if we define, for $\mathbf{a} \in \mathsf{R}^T$, $m_\mathbf{a} = \min_t a_t$, $M_\mathbf{a} = \max_t a_t$, $N_\mathbf{x} = N_X$ and $N_\mathbf{y} = N_Y$, we can write

$$P' = \{(i, j) \in P : L_\mathbf{x} \le i \le U_\mathbf{x} \text{ and } L_\mathbf{y} \le j \le U_\mathbf{y}\},$$

where, for $\mathbf{a} = \mathbf{x}, \mathbf{y}$,

$$L_\mathbf{a} = I_{]-\infty,0[}(m_\mathbf{a})(1 - m_\mathbf{a}) + I_{[0,+\infty[}(m_\mathbf{a}),$$

and

$$U_\mathbf{a} = I_{]-\infty,0[}(M_\mathbf{a})N_\mathbf{a} + I_{[0,+\infty[}(M_\mathbf{a})(N_\mathbf{a} - M_\mathbf{a}),$$

with I_A standing for the indicator function of the generic set A.

The model set through equations (1) and (2) belongs to the general framework usually applied in image restoration analyses, where, as discussed by Cressie (1993, p. 499), for the ground truth $\mathbf{S}' = (S_{1,1} \quad \cdots \quad S_{N_X,N_Y})$ and the corrupted image $\mathbf{Z}' = (Z_{m_\mathbf{x},m_\mathbf{y}} \quad \cdots \quad Z_{M_\mathbf{x},M_\mathbf{x}})$ the following is assumed to hold:

$$Z_{i,j} = \phi\left(\sum\nolimits_{(c_1,c_2)\in P} H(i - c_1, j - c_2) S_{c_1,c_2}\right) \oplus \varepsilon_{i,j} \tag{3}$$

where ϕ is a any function, H is a blurring matrix corresponding to a point-spread function such that $f_{H,i,j}(\mathbf{S}) = \sum_{(c_1,c_2)\in P} H(i - c_1, j - c_2) S_{c_1,c_2}$ is translation-invariant, ε is a white noise and $\oplus$ is an invertible operator (Geman and Geman, 1984). To see how model (1)-(2) can be considered a specialization of (3), we request linearity for ϕ and interpret $\oplus$ as addition. Furthermore, for $(\nu_1, \nu_2) \in \mathsf{Z}^2$ we define

$$H^*(\nu_1, \nu_2) = \begin{cases} \theta_t & \text{if } (\nu_1, \nu_2) = (-x_t, -y_t) \text{ for some } t \in \{1, \ldots, T\} \\ 0 & \text{otherwise} \end{cases} \tag{4}$$

and observe that, under condition (2), f_{H^*} is translation invariant as required, since $f_{H^*,i,j}(\mathbf{S} + \mathbf{1}\delta) = \sum_{t=1}^{T} \theta_t (S_{i+x_t,j+y_t} + \delta) = f_{H^*,i,j}(\mathbf{S}) + \delta$ for every real δ.

The explanation of the error propagation on spatial correlation measures needs further assumptions in addition to (1) and (2). In particular, we assume, as in Arbia and Haining (1993), the following conditions on spatial drifts and correlation functions of $S_{i,j}$ and $\varepsilon_{i,j}$.

For every pair (i, j) in P,

$$\mathrm{E}(\varepsilon_{i,j}) = 0$$

and

$$\mathrm{Var}(\varepsilon_{i,j}) = \sigma_\varepsilon^2 .$$

For every pair of integers $(k,h) \neq (0,0)$ such that $(i+k, j+h) \in P$,

$$\mathrm{Cov}(\varepsilon_{i,j}, \varepsilon_{i+k,j+h}) = 0.$$

For every pair (i,j) in P and (k,h) such that $(i+k, j+h) \in P$,

$$\mathrm{Cov}(\varepsilon_{i,j}, S_{i+k,j+h}) = 0,$$

$$\mathrm{E}(S_{i,j}) = \mu ,$$

and

$$\mathrm{Cov}(S_{i,j}, S_{i+k,j+h}) = \sigma_S^2 \rho(\|(k,h)\|) ,$$

where $\rho(\|(k,h)\|)$, is an isotropic "ground truth" spatial correlation function at distance $\|(k,h)\|$.

These assumptions enable us to determine the theoretical spatial correlation between pairs of observed, error-corrupted, variates $Z_{i,j}$ and $Z_{i+k,j+h}$ in cases when $(i,j) \in P'$ and the pair (k,h) is such that the related pair $(i+k, j+h)$ also belongs to the lattice P'. More thoroughly, our view is that there are two sources of spatial dependence among neighboring pixels. The first source can be attributed to the intrinsic continuity of phenomena in space, which we take into account by defining $S_{i,j}$ as a spatially autocorrelated process. The second one, due to a displacement error for which the recording sensor assigns a reflectance value to a pixel by averaging the values corresponding to its neighborhood, is assessed in our context by using the weighting scheme $(S_{i+x_1,j+y_1} \quad \cdots \quad S_{i+x_T,j+y_T})\boldsymbol{\theta}$ in model (3). Our aim is to identify the "ground truth" spatial correlations, i.e. those characterizing $S_{i,j}$, from the sample correlation estimates based on $Z_{i,j}$, which nevertheless convey information from both the dependency sources we deal with. To do so, let us define, for $(i,j) \in P$ and $(k,h) \in \mathbb{N}^2$ such that $(i+k+x_t, j+h+y_t) \in P$ for all $t = 1,\ldots,T$, the vectors

$$\mathbf{s}'_{k,h}(i,j) = (S_{i+x_1,j+y_1} \quad \cdots \quad S_{i+x_T,j+y_T}) .$$

Furthermore, let **B** be the matrix $\begin{pmatrix} \phi_1\boldsymbol{\theta}' & 1 & \mathbf{0}' & 0 \\ \mathbf{0}' & 0 & \phi_1\boldsymbol{\theta}' & 1 \end{pmatrix}$ and $\mathbf{g}_{k,h}(i,j)$ the vector

$(\mathbf{s}'_{0,0}(i,j) \quad \varepsilon_{i,j} \quad \mathbf{s}'_{k,h}(i,j) \quad \varepsilon_{i+k,j+h})'$.

In this way, the variates $Z_{i,j}$ and $Z_{i+k,j+h}$ can be written as

$$\begin{pmatrix} Z_{i,j} \\ Z_{i+k,j+h} \end{pmatrix} = \begin{pmatrix} \phi_0 \\ \phi_0 \end{pmatrix} + \mathbf{B}\mathbf{g}_{k,h}(i,j),$$

and, correspondingly, their covariance matrix admits the expression

$$\mathrm{Cov}\begin{pmatrix} Z_{i,j} \\ Z_{i+k,j+h} \end{pmatrix} = \mathbf{B}\mathrm{Cov}(\mathbf{g}_{k,h}(i,j))\mathbf{B}'. \tag{5}$$

If we now consider the function $\mathbf{R}: \mathbb{Z}\times\mathbb{Z} \to \mathbb{R}^{\{1,\dots,T\}^2}$ defined as follows

$$\mathbf{R}(k,h) = \begin{pmatrix} \rho_{k,h} & \rho_{k+x_2-x_1,h+y_2-y_1} & \cdots & \rho_{k+x_T-x_1,h+y_T-y_1} \\ \rho_{k+x_1-x_2,h+y_1-y_2} & \rho_{k,h} & \cdots & \rho_{k+x_T-x_2,h+y_T-y_2} \\ \vdots & \vdots & \ddots & \vdots \\ \rho_{k+x_1-x_T,h+y_1-y_T} & \rho_{k+x_2-x_T,h+y_2-y_T} & \cdots & \rho_{k,h} \end{pmatrix},$$

with "$\rho_{k,h}$" the short for "$\rho(\|(k,h)\|)$", we are able to derive:

$$\mathrm{Cov}(\mathbf{g}_{k,h}(i,j)) = \sigma_S^2 \begin{pmatrix} \mathbf{R}(0,0) & \mathbf{0} & \mathbf{R}(k,h) & \mathbf{0} \\ \mathbf{0}' & snr^{-1} & \mathbf{0}' & 0 \\ \mathbf{R}(k,h) & \mathbf{0} & \mathbf{R}(0,0) & \mathbf{0} \\ \mathbf{0}' & 0 & \mathbf{0}' & snr^{-1} \end{pmatrix}, \tag{6}$$

where, in addition to the previous notation, $snr = \sigma_S^2 / \sigma_\varepsilon^2$ is the signal-to-noise ratio (see Campbell, 1996). Finally, using (5) and (6), after some algebra the (observed) spatial covariances can be expressed as:

$$Cov\begin{pmatrix} Z_{i,j} \\ Z_{i+k,j+h} \end{pmatrix} = \sigma_S^2 \begin{pmatrix} \phi_1^2\boldsymbol{\theta}'\mathbf{R}(0,0)\boldsymbol{\theta} + snr^{-1} & \phi_1^2\boldsymbol{\theta}'\mathbf{R}(k,h)\boldsymbol{\theta} \\ \phi_1^2\boldsymbol{\theta}'\mathbf{R}(k,h)\boldsymbol{\theta} & \phi_1^2\boldsymbol{\theta}'\mathbf{R}(0,0)\boldsymbol{\theta} + snr^{-1} \end{pmatrix}. \tag{7}$$

Equation (7) relates second order moments of the corrupted process Z to the correlation structure, represented by the **R** function, of the "ground truth" process S. Such relationship is parametric with respect to the technical characteristics of the sensor's device, and can be explicitly exploited to correct spatial correlation estimates based on Z's observations whenever enough knowledge on the location error (parameters $\boldsymbol{\theta}$ and ϕ_1) and of the measurement error (parameter *snr*) is available. To illustrate how the correction can be executed, let us assume that a vector of correlation estimates $\mathbf{r}(m) = (r_{1,0} \quad \cdots \quad r_{m,m})'$ is obtained from the observed map Z for spatial lags (k,h) in the set

$$Q(m) = \bigcup_{k=1}^{m} \{(k,h) : h = 0,\dots,k\},$$

with $m > 1$, and define set $Q^* = \{(k_1,h_1),\dots,(k_{|Q^*|},h_{|Q^*|})\}$ as the largest subset of $Q(m)$ for which if lag (k,h) is in Q^* then every correlation ρ_{c_1,c_2} in $\mathbf{R}(k,h)$ is such that $(c_1,c_2) \in Q(m)$. In addition, we require that every component ρ of $\mathbf{R}(0,0)$ also corresponds to a lag in $Q(m)$, and define the system

$$\begin{aligned} r_{k_1,h_1} &= \phi_1^2 \boldsymbol{\theta}' \mathbf{R}(k_1,h_1)\, \boldsymbol{\theta} / (\phi_1^2 \boldsymbol{\theta}' \mathbf{R}(0,0)\, \boldsymbol{\theta} + snr^{-1}) \\ &\;\;\vdots \\ r_{k_{|Q^*|},h_{|Q^*|}} &= \phi_1^2 \boldsymbol{\theta}' \mathbf{R}(k_{|Q^*|},h_{|Q^*|})\, \boldsymbol{\theta} / (\phi_1^2 \boldsymbol{\theta}' \mathbf{R}(0,0)\, \boldsymbol{\theta} + snr^{-1}) \end{aligned} \tag{8}$$

whose equations are deduced applying formula (7) for every lag in Q^*.

System (8) can be interpreted as a set of $|Q^*|$ nonlinear constraints which are imposed to a vector $\boldsymbol{\varrho}^*$ of say n variables which are given by all those correlation measures which correspond to distinct entries in matrices $\mathbf{R}(0,0)$, $\mathbf{R}(k_1,h_1)$, ..., $\mathbf{R}(k_{|Q^*|},h_{|Q^*|})$. To correct the error introduced by the remote data acquisition, we henceforth propose to solve the system numerically using the corresponding vector of correlation estimates $\mathbf{r}^*$ as the starting solution to (8).

Although the procedure can be executed for every value of ϕ_1, $\boldsymbol{\theta}$, $\mathbf{x}$, $\mathbf{y}$ and *snr*, in the sequel we will focus on Landsat characteristics (Welsh *et al.*, 1985) by setting

$$\phi_0 = 0, \quad \phi_1 = 1, \quad \mathbf{x}' = (0 \quad 1 \quad 0 \quad 1), \quad \mathbf{y}' = (0 \quad 0 \quad 1 \quad 1), \tag{9}$$

and constraining the parameters' vector $\boldsymbol{\theta}$ by imposing

$$\theta_2 = \theta_3 = \sqrt{\theta_1} - \theta_1, \quad \theta_4 = (1 - \sqrt{\theta_1})^2, \tag{10}$$

so that equation (2) holds true and the location error is taken into account by using just a single parameter, θ_1, that increases when location error diminishes:

$$Z_{i,j} = \theta_1 S_{i,j} + (\sqrt{\theta_1} - \theta_1)(S_{i+1,j} + S_{i,j+1}) + (1 - \sqrt{\theta_1})^2 S_{i+1,j+1} + \varepsilon_{i,j} \tag{11}$$

Under condition (9), system (8) is formed by $|Q(m-1)|$ relations on $|Q(m)|$ variables with $\boldsymbol{\varrho}^* = (\rho_{1,0} \quad \cdots \quad \rho_{m,m})'$ and $\mathbf{r}^* = \mathbf{r}(m)$, where

$$|Q(m)| = m\frac{m+3}{2}, \quad m > 0,$$

or, recursively,

$$|Q(m)| = |Q(m-1)| + m + 1,$$

since we can write

$$\mathbf{r}(m) = (\mathbf{r}(m-1)' \quad (r_{m,0} \quad \cdots \quad r_{m,m}))'.$$

As previously observed, we need to specify the amount of location and measurement error typical of the sensor device employed to acquire the data. In order to represent real world empirical circumstances, we henceforth decide to implement the procedure focusing on typical quantifications of the location and measurement errors. In particular, when using Landsat data the location error has been quantified by Welsh *et al.* (1985) to the value $\theta_1 = 0.5$, even if new sensors used on more recent satellite programs dramatically improve location precision (see Landsat, 2000). Dealing with measurement errors, a detailed list of the *snr*'s associated with various last generation sensor devices can also be found in Landsat (2000). Notwithstanding, Short (1999) quantifies the noise of the sensors of the most recent satellites (ETM+ sensor) to a value of $snr^{-1} = 0.05$. For these reasons in the following sections we will analyze the correcting procedure by emphasizing its behavior under the hypotheses $\theta_1 = 0.5$ and $snr^{-1} = 0.05$.

3. THEORETICAL EXAMPLE: CORRECTING THE NEGATIVE EXPONENTIAL CORRELOGRAM

In this section we discuss the effects of the proposed correction technique using the negative exponential function to model the ground truth correlogram (Matern, 1986). Explicitly, at lag (k,h) we have

$$\rho(\|(k,h)\|) = \exp(-\beta\|(k,h)\|) \tag{12}$$

with β the parameter that controls for decay ($\beta > 0$). More thoroughly, our illustrative examples deal with two correlation functions defined by setting in (12) $\beta = 0.15$ and $\beta = 0.75$, which respectively represent strong and weak spatial dependency cases. Under parametrization (10) we can give, for model (11), a more explicit, scalar expression to $\mathrm{Var}(Z_{i,j})$ and $\mathrm{Cov}(Z_{i,j}, Z_{i+k,j+h})$, since, by defining $A = \theta_1^2 + (1-\sqrt{\theta_1})^4 + 2(\sqrt{\theta_1} - \theta_1)^2$, $B = 4(\theta_1 + (1-\sqrt{\theta_1})^2)(\sqrt{\theta_1} - \theta_1)$ and $C = 4\theta_1(1-\sqrt{\theta_1})^2$, we can write, using (7),

$$\mathrm{Var}(Z_{i,j}) = A + B\rho_{0,1} + C\rho_{1,1} + snr^{-1}, \tag{13}$$

and

$$\begin{aligned}\mathrm{Cov}(Z_{i,j}, Z_{i+k,j+h}) = A\rho_{k,h} &+ (B/4)(\rho_{k+1,h} + \rho_{k-1,h} + \rho_{k,h+1} + \rho_{k,h-1}) \\ &+ (C/4)(\rho_{k+1,h+1} + \rho_{k-1,h-1} + \rho_{k-1,h+1} + \rho_{k+1,h-1}),\end{aligned} \tag{14}$$

where σ_S^2 is conventionally assumed equal to 1.

If the ground truth correlation structure is assumed as known, then the performance of the procedure can be investigated from a theoretical point of view as follows. At a first step we calculate the RHS of Formulae (13) and (14) for given values of θ_1 and *snr*, thus obtaining the covariance function of the corrupted map *Z*. Figures 1 and 2 show how location and attribute errors distort the spatial correlogram up to lag $(3,3)$ under model (11), respectively for β = 0.15 (strong dependency) and β = 0.75 (weak dependency), when $\theta_1 \in \{0.3, 0.5\}$ and $snr^{-1} \in \{0.01, 0.05, 0.10\}$. It can be noted that the observed correlations generally increase for increasing location errors and decreasing measurement errors, i.e. when snr^{-1} or θ_1 decrease. Furthermore, the effects of attribute errors are relatively greater than those due to location errors. For highly correlated data (see Figure 1), errors tends to be constant and the correlation measures obtained using the corrupted map *Z* overestimate the ground truth correlations except in the case when $\theta_1 = 0.5$ and $snr^{-1} = 0.10$. In contrast, if data are weakly correlated (see Figure 2), errors tend to vanish for increasing spatial lags, especially when $\|(k,h)\| > 2$, and the observed correlations always overestimate the corresponding ground truth measures.

The correlation functions obtained in the previous step can now be interpreted as the "observed" correlograms, which can henceforth be used as the starting point of the correction process described in Section 2. Figures 3 and 4 show how location and attribute errors can be corrected under model (11), respectively for β = 0.15 (strong dependency), and β = 0.75 (weak dependency), when $\theta_1 \in \{0.3, 0.5\}$ and $snr^{-1} \in \{0.01, 0.05, 0.10\}$. It can be seen that the procedure achieves a perfect rectification in plot B of Figure 4, i.e. when the true spatial correlation is weak and rapidly declining (β = 0.75), and a good rectification in plot A (moderately declining spatial correlation) only if, in addition, $snr^{-1} = 0.10$. In contrast, the procedure does not achieve a satisfactory correction in cases when data are highly correlated (see Figure 3) or, for the weak dependency case, when a high location error occurs ($\theta_1 = 0.3$) and, furthermore, $snr^{-1} > 0.10$.

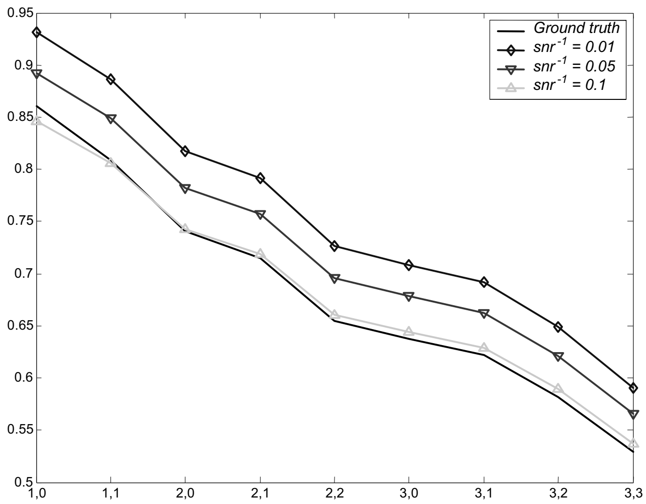

A: $\theta_1 = 0.3$

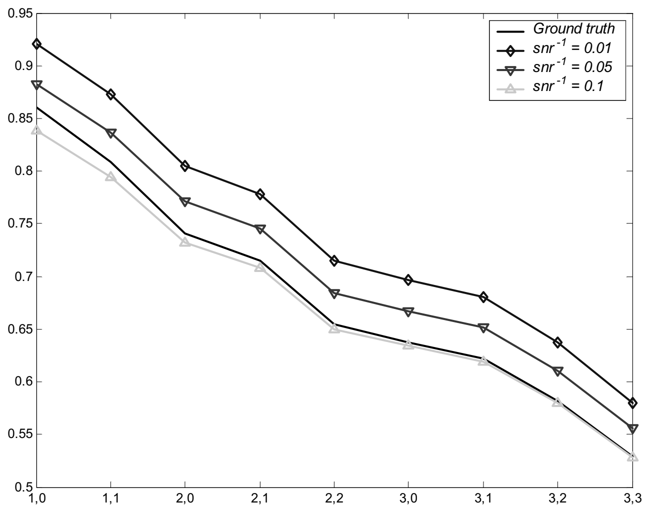

B: $\theta_1 = 0.5$

Figure 1 – Spatial correlation distortions in the remotely acquired images for various values of location and attribute error parameters (θ_1 and *snr*), under model (11), for the strong dependency case ($\beta = 0.15$ in equation (12)). Error-corrupted correlations are reported in the graph for spatial lags (*k*,*h*), *k*,*h* = 0, ..., 3, when snr^{-1}=0.01, 0.05, 0.1, $\theta_1 = 0.3$ (Plot A), and $\theta_1 = 0.5$ (Plot B).

4. ASSESSING CORRECTION EFFICIENCY VIA MONTE CARLO SIMULATION OF SAR MAPS

In this section we investigate the efficiency of the error-corrected correlation measures with respect to those ones based on the application of the Method-of-Moments estimator to maps corrupted following model (11), with $\theta_1 = 0.5$ and $snr^{-1} = 0.05$, by designing a Monte Carlo experiment to generate images on a grid of 30x30 pixels from an isotropic SAR process (see - e.g. - Cressie, 1993), which,

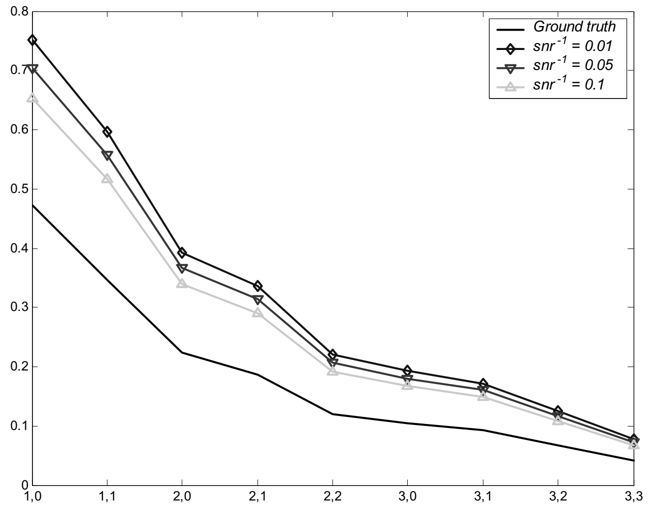

A: $\theta_1 = 0.3$

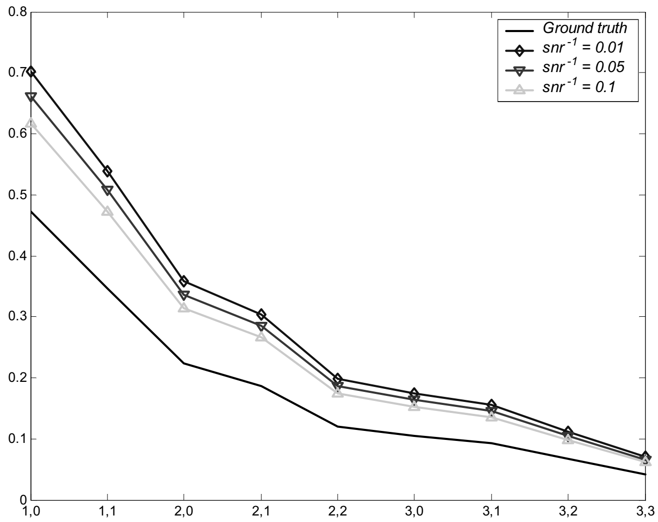

B: $\theta_1 = 0.5$

Figure 2 – Spatial correlation distortions in the remotely acquired images for various values of location and attribute error parameters (θ_1 and *snr*), under model (11), for the weak dependency case (β = 0.75 in equation (12)). Error-corrupted correlations are reported in the graph for spatial lags (k,h), k,h = 0, ..., 3, when snr^{-1}=0.01, 0.05, 0.1, θ_1 = 0.3 (Plot A), and θ_1 = 0.5 (Plot B).

as discussed by Benedetti and Espa (1993), is simulated by filtering a Gaussian white noise laid on the selected lattice.

As in Section 3, we consider again two degrees of spatial dependency for the "ground truth" by selecting different convolution kernels in SAR simulations (see Arbia *et al.*, 1999), namely we define "strong" dependency when the weights of the mask filter are set as follows:

$$w_{i,j} = 0.8849 \exp(-1.5 d_{i,j}) \quad i, j \in \{1,\ldots,5\}$$

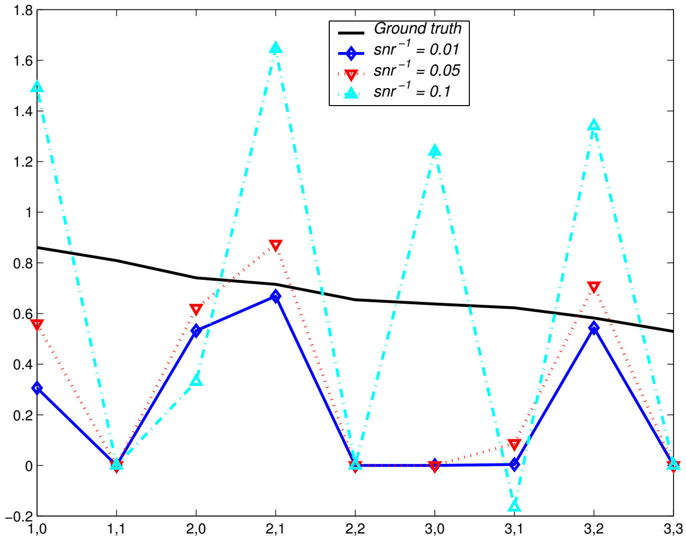

A: $\theta_1 = 0.3$

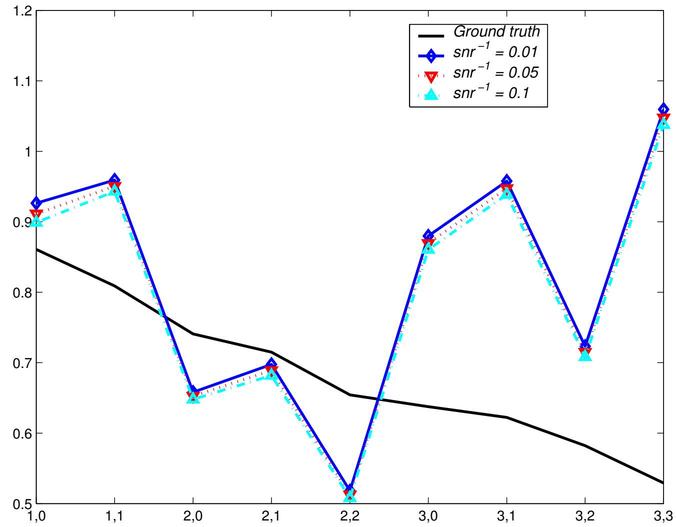

B: $\theta_1 = 0.5$

Figure 3 – Corrected correlation estimates for various values of location and attribute error parameters (θ_1 and snr), under model (11), for the strong dependency case ($\beta = 0.15$ in equation (12)). Correlations are reported in the graph for spatial lags (k,h), k,h = 0, ..., 3, when snr^{-1}=0.01, 0.05, 0.1, θ_1 = 0.3 (Plot A), and θ_1 = 0.5 (Plot B).

and "weak" dependency by setting

$$w_{i,j} = 0.4438\exp(-0.5d_{i,j}) \quad i, j \in \{1,\ldots,5\},$$

where $d_{i,j}$ is the distance between the pixel at the centre of the filter and the pixel in position i,j in the filter.

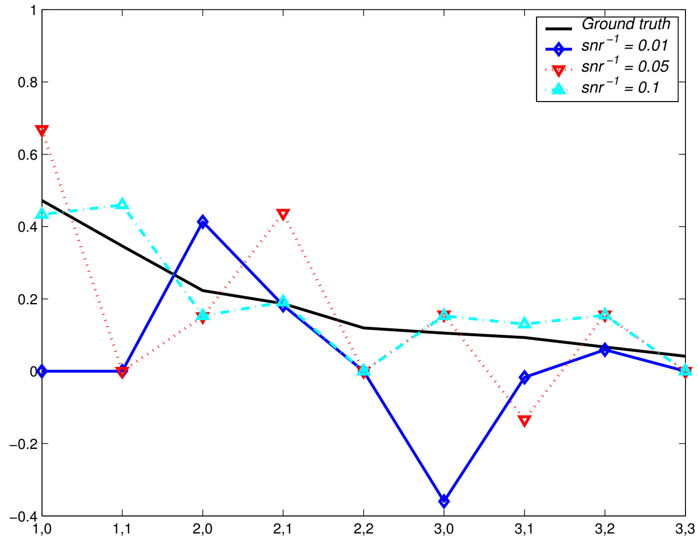

A: $\theta_1 = 0.3$

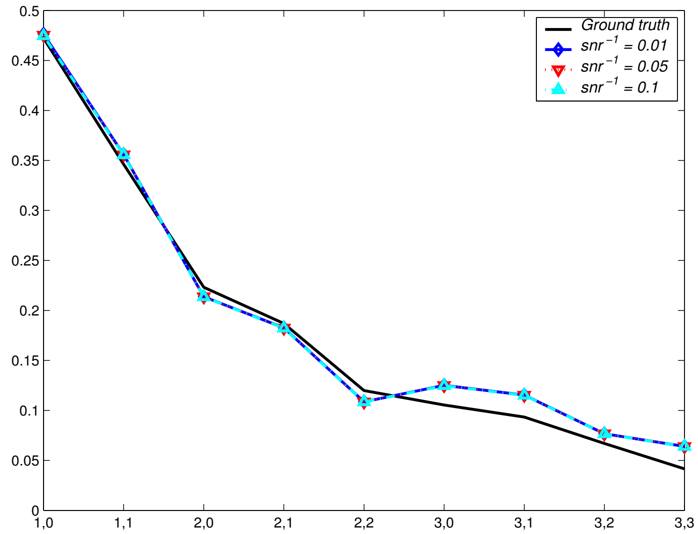

B: $\theta_1 = 0.5$

Figure 4 – Corrected correlation estimates for various values of location and attribute error parameters (θ_1 and *snr*), under model (11), for the weak dependency case ($\beta = 0.75$ in equation (12)). Correlations are reported in the graph for spatial lags (*k*,*h*), *k*,*h* = 0, ..., 3, when snr^{-1}=0.01, 0.05, 0.1, θ_1 = 0.3 (Plot A), and θ_1 = 0.5 (Plot B).

For each of the two correlation structures defined above, to obtain reliable Monte Carlo estimates we generate - as suggested by Haining and Arbia (1993) - a number of 300 images, say ${}_mS_{i,j}$, $m = 1,\ldots,300$. For every *m*, the SAR map ${}_mS$ is thus corrupted in order to obtain the corresponding "observed" map ${}_mZ$, and, relying on such ${}_mZ$'s, spatial correlations are estimated up to lag (5,5) by making use of a classical Method-of-Moments covariogram estimator (MM) (see, for example, Cressie, 1993, eq. 2.4.4), say obtaining measures ${}_m\hat{\rho}_{k,h}$ for $(k,h) \in Q(5)$. Such estimates were henceforth corrected up to lag $(4,4)$ as described in Section 2 by setting $r_{k,h} = {}_m\hat{\rho}_{k,h}$ in the LHS of (8) and using vector $({}_m\hat{\rho}_{1,0} \quad \cdots \quad {}_m\hat{\rho}_{5,5})$ in the RHS as the starting point of the optimizer, whose solution at convergence is here indicated for the *m*-th map as ${}_m\tilde{\rho}_{k,h}$ and referred to as the Corrected Method-of-Moments estimator (CMM).

We measure the efficiency of the $\tilde{\rho}$'s and the $\hat{\rho}$'s estimates on a lag by lag basis by estimating the corresponding Root Mean Square Errors as follows

$$\text{RMSE}(\rho_{\text{Est},k,h}) = \sqrt{\frac{1}{300}\sum_{m=1}^{300}({}_m\rho_{\text{Est},k,h} - \rho_{k,h})^2} \tag{15}$$

where $\rho_{k,h}$ are the "true" correlations induced by the applied filters and $\rho_{\text{Est},k,h}$ is $\hat{\rho}_{k,h}$ or $\tilde{\rho}_{k,h}$. Furthermore, the efficiency of the $\tilde{\rho}$ estimator is compared to that of the $\hat{\rho}$ estimator by means of the following index:

$$\text{RelEff}(k,h) = 100\frac{\text{RMSE}(\tilde{\rho}_{k,h})}{\text{RMSE}(\hat{\rho}_{k,h})}. \tag{16}$$

Table 1 shows the results we obtain applying Formulae (15) and (16) for the strong dependency case. It can be noted that the procedure is inefficient excepting for corrections corresponding to high lags. In Table 2 are reported efficiency evaluations executed for the weak dependency case. We observe that, under this assumption, the procedure is very efficient at all lags excluding lag $(3,3)$.

TABLE 1

Root mean square errors for the classical (MM) and the corrected (CMM) method-of-moments estimators of spatial correlations at lags (1,0), ..., (4,4) under the strong dependency case.
The relative efficiency between the considered estimators is reported using the RelEff statistic (see eq. (16))

	Spatial lag						
	1,0	1,1	2,0	2,1	2,2	3,0	3,1
CMM Estimator	0.0675	0.0748	0.0497	0.0691	0.0616	0.0996	0.1152
MM Estimator	0.0282	0.0334	0.0461	0.0522	0.0661	0.0652	0.0692
RelEff	239.4218	224.3841	107.8173	132.1804	93.2079	152.7584	166.4253

	Spatial lag						
	3,2	3,3	4,0	4,1	4,2	4,3	4,4
CMM Estimator	0.0926	0.1690	0.0926	0.0793	0.0569	0.0320	0.0125
MM Estimator	0.0756	0.0844	0.0732	0.0741	0.0778	0.0868	0.0928
RelEff	122.5116	200.3498	126.5013	107.0916	73.1569	36.8585	13.4287

Figures 5 and 6 show the correlogram estimates - averaged map by map - for the cases of strong and weak dependency respectively. When the spatial correlation is strong, Figure 5 shows that there's no point in correcting the MM esti-

TABLE 2

Root mean square errors for the classical (MM) and the corrected (CMM) method-of-moments estimators of spatial correlations at lags (1,0), ..., (4,4) under the weak dependency case.
The relative efficiency between the considered estimators is reported using the RelEff statistic (see eq. (16))

	Spatial lag						
	1,0	1,1	2,0	2,1	2,2	3,0	3,1
CMM Estimator	0.0541	0.0512	0.0416	0.0438	0.0393	0.0580	0.0536
MM Estimator	0.1633	0.1461	0.0986	0.0838	0.0590	0.0601	0.0529
RelEff	33.1277	35.0355	42.1487	52.3010	66.5823	96.5418	101.3689

	Spatial lag						
	3,2	3,3	4,0	4,1	4,2	4,3	4,4
CMM Estimator	0.0467	0.0789	0.0042	0.0035	0.0021	0.0008	0.0002
MM Estimator	0.0489	0.0524	0.0506	0.0466	0.0443	0.0497	0.0540
RelEff	95.5348	150.5376	8.2683	7.5467	4.6992	1.5923	0.3104

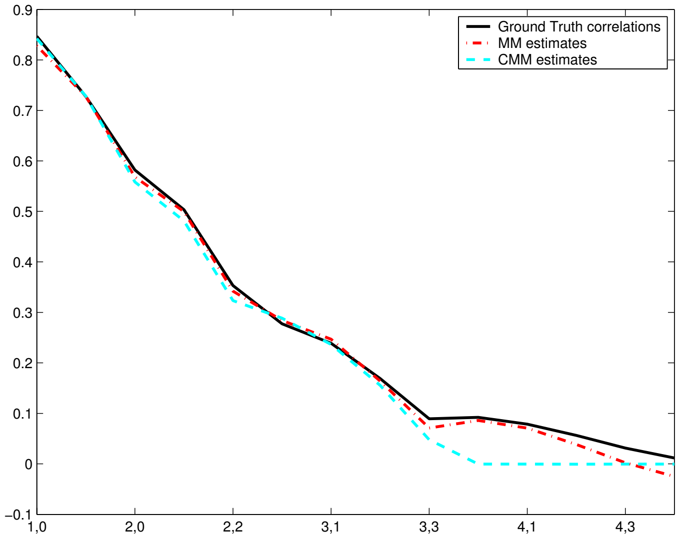

Figure 5 – Mean correlation measures under the strong dependency case for the classical (MM) and the corrected (CMM) Method-of-Moments estimators.

mates, as they actually coincide, on average, with the corresponding CMM ones. On the contrary, for weak correlations the procedure really corrects the MM estimates at all lags up to lag (3,3) .

5. DISCUSSION AND CONCLUDING REMARKS

In this paper we propose a procedure for the error-correction of spatial correlation estimates based on remotely sensed data. The proposed procedure has proved to work pretty well in a set of simulated cases in which we allowed location error, attribute error and spatial correlation to assume a set of values in a real world representative range. The cases where the results are not satisfactory are

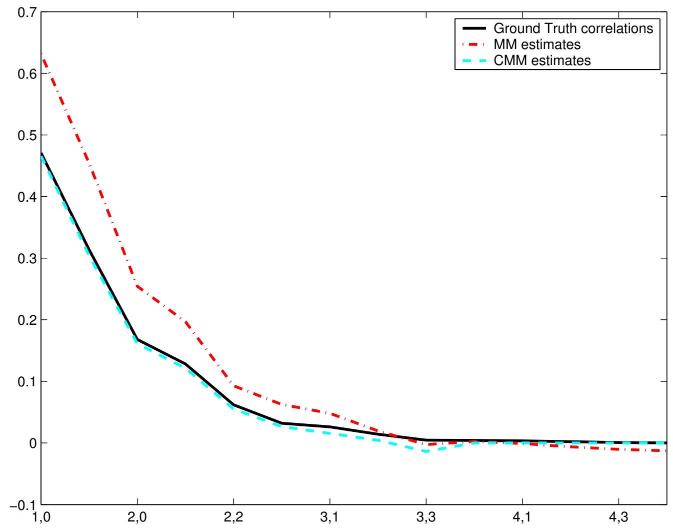

Figure 6 – Mean correlation measures under the weak dependency case for the classical (MM) and the corrected (CMM) Method-of-Moments estimators.

instead those where the location error is very high ($\theta_1 < 0.3$) and furthermore the true landscape is characterized by strong and slowly declining correlation function. It should be remarked, however, that the values of the location error that dramatically distort the image and disprove the procedure are by far smaller than the limits observed by Welsh *et al.* (1985) for Landsat data. As a consequence, these situations appear to be extremely unlikely in empirical cases. In addition, for the strong dependency case in which the procedure doesn't work properly, the Method-of-Moments estimator simply doesn't need to be corrected, since its estimates are actually equal to the corresponding corrected ones, as can be observed inspecting Figure under the SAR assumption.

The procedure proposed here is very general and can be easily adapted to every corruption model in the class defined by equation (3). In particular, improvements in the sensor device's measurement characteristics can also be taken into account by setting the correct signal-to-noise ratio. It's worth noting that, as showed in Figures 1 and 2, a better signal corresponds to a worse distortion in the estimated correlations, so that enhancements in the remote sensing technology will still emphasize the needs for a careful correction of satellite-based dependency measures.

Department of Business, Statistical, Technological and Environmental Scienes (DASTA)
"G. d'Annunzio" University

GIUSEPPE ARBIA
GIOVANNI LAFRATTA

REFERENCES

G. ARBIA, (1993), *The use of GIS in spatial statistical survey*, "International Statistical Review", 61, 2, pp. 339-359.

G. ARBIA, R. BENEDETTI, G. ESPA, (1999), *Contextual classification in image analysis: an assessment of accuracy of ICM*, "Computational Statistics & Data Analysis", 30, pp. 443-455.

G. ARBIA, D. GRIFFITH, R. HAINING, (1998), *Error propagation modelling in raster GIS: overlay operations*, "International Journal of Geographical Information Science", 12, pp. 145-167.

G. ARBIA, D. GRIFFITH, R. HAINING, (1999), *Error propagation modelling in raster GIS: addition and ratioing operations*, "Cartography & Geographical Information Science", 26, pp. 297-315.

G. ARBIA, G. LAFRATTA, (1997), *Evaluating and updating the sample design in repeated environmental surveys: monitoring air quality in Padua*, "Journal of Agricultural, Biological and Environmental Statistics", 2, 4, pp. 451-466.

G. ARBIA, G. LAFRATTA, (2002), *Anisotropic spatial sampling designs for urban pollution*, "Journal of the Royal Statistical Society", C Series, 51, 2, pp. 223-234.

R. BENEDETTI, G. ESPA, (1993), *Alcuni metodi per la generazione di processi aleatori bidimensionali*, "Statistica Applicata", 5, 3, pp. 217-244.

J.B. CAMPBELL, (1996), *Introduction to remote sensing*, second edition, The Guilford Press, New York.

N.A.C. CRESSIE, (1993), *Statistics for spatial data*, Wiley, New York.

S. GEMAN, D. GEMAN, (1984), *Stochastic relaxation, Gibbs distributions and the Bayesian restoration of images*, "IEEE Transactions in Pattern Analysis and Machine Intelligence", 6, pp. 721-742.

R. HAINING, G. ARBIA, (1993), *Error propagation through map operations*, "Technometrics", 35, pp. 293-305.

LANDASAT, (2000), http://eo1.gsfc.nasa.gov/technology/documents/instrumentoverview.html.

B. MATERN, (1986), *Spatial variation*, Second Edition, Lectures Notes in Statistics, 36, Springer, New York.

N.M. SHORT, (1999), *Remote sensing tutorial*, NASA publications, http://rst.gsfc.nasa.gov/Front/Start.html.

R. WELSCH, T.R. JORDAN, M. EHLERS, (1985), *Comparative evaluations of the geodetic accuracy and cartographic potential of Landsat-4 and Landsat-5 thematic mapper image data*, "Photogrammetric engineering and remote sensing", 51, pp. 1799-1812.

RIASSUNTO

Stime della correlazione spaziale da osservazioni satellitari corrette sulla base delle caratteristiche tecniche del sensore

In molti studi empirici le misure di correlazione spaziale basate su dati satellitari sono utilizzate per identificare la distanza oltre la quale la dipendenza tra fenomeni risulta non rilevante, per assistere, ad esempio, nella scelta della localizzazione di griglie sistematiche nelle indagini campionarie a terra. Tuttavia, le stime così ottenute sono minate dal fatto che l'inferenza si basa su dati che, raccolti via satellite, costituiscono solo un'approssimazione della "verità a terra", a causa della presenza di una serie di fattori di disturbo quali, ad esempio, la rifrazione ottica, la presenza di ostacoli (quali i corpi nuvolosi) e le limitazioni della precisione degli strumenti disponibili. In questo lavoro viene introdotta una procedura per correggere la stima della correlazione spaziale utilizzando l'informazione disponibile a priori circa le caratteristiche tecniche del sensore satellitare, migliorando così l'attendibilità delle stime. Si propone un'approssimazione della "reale" correlazione in funzione delle stime basate sul satellite e delle caratteristiche tecniche del sistema satellitare stesso. Gli effetti di tali interventi correttivi sono discussi facendo riferimento ad una serie di esempi basati su un correlogramma teorico di tipo isotropico negativamente esponenziale. L'efficienza con cui la procedura di correzione opera relativamente allo stimatore del metodo dei momenti è stata infine valutata attraverso un esperimento Monte Carlo in cui si è ipotizzato un processo SAR per la generazione delle mappe rappresentative della "verità a terra".

SUMMARY

Spatial correlation estimates based on satellite observations corrected with the prior knowledge on sensor devices' technical characteristics

In many empirical studies spatial correlations are used to identify the distance above which dependency is negligible, to assist the choice in locating a systematic grid of sample points in ground surveys. However, estimates are undermined by the fact that our inference is based on satellite data that are only an approximation of the ground truth, due to the presence of a series of disturbing factors like (e.g.) light scattering, presence of obstacles (like clouds), and instrument precision limitations. In this paper we introduce a procedure to correct spatial correlation estimates using prior knowledge on the satellite sensor's technical characteristics and obtain more reliable estimates. We derive an approximation of the "ground-truth" pattern of correlation as a function of the satellite-based spatial correlation and of the sensor's (user-specified) technical characteristics. We show the effects of these corrections referring to a series of illustrative examples based on theoretical calculations regarding the negative exponential correlogram. The correction efficiency relative to the classical Method-of-Moments estimator is also assessed by means of a Monte Carlo application to simulated SAR maps.